

Erdheim-Chester 病の肺病変について

研究分担者： 小倉 高志（神奈川県立循環器呼吸器センター副院長兼呼吸器内科部長）
馬場 智尚（同センター呼吸器内科医長）
泉 信有（国立国際医療センター呼吸器内科）

研究要旨

Erdheim-Chester 病は、肺病変の合併は 20-50%に認められ、胸部 CT では小葉間隔壁の肥厚、小葉中心性の結節、スリガラス状濃度上昇、胸水を伴うと報告されている。今回の疫学的調査では集積した 40 例のうち肺病変の合併は 11 例であり、呼吸器症状を有した例は 8 例であった。胸部 CT では、小葉間隔壁の肥厚（6 例）、小葉中心性結節性陰影（2 例）、嚢胞形成（4 例）、胸膜肥厚（4 例）であった。Erdheim-Chester 病の CT 画像所見として、小葉間隔壁の肥厚は特徴的であり、リンパ路にそった病変の進展が考えられた。

A. 研究目的

Erdheim-Chester 病の肺病変について、その臨床像と画像所見を明らかにする事。

B. 研究方法

アンケートによる疫学的調査の解析から、Erdheim-Chester 病の肺病変についても検討する。
（倫理面の配慮）人権擁護上、対象者に対する配慮が必要である。当研究では疫学研究に関する倫理指針、臨床研究に関する倫理指針を遵守する。臨床情報は施設の定める手続きに従い匿名化を行った上で扱う。以上の体制により、研究の安全性および倫理的妥当性が確保される。

C. 研究結果

今回の疫学的調査では解析した 38 例のうち肺病変の合併は 11 例であり、呼吸器症状を有した例は 8 例であった。

胸部 CT を検討できた 11 例では、小葉間隔壁の肥厚（6 例）、小葉中心性結節性陰影（2 例）、嚢胞形成（4 例）、胸膜肥厚（4 例）であった。

典型的画像と対応する病理像を示す。

図 1

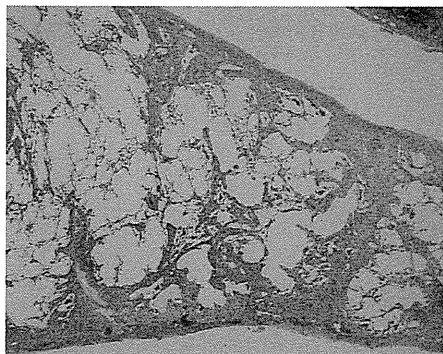


（患者 1）胸部 HR-CT 像。小葉間隔壁の肥厚が目立つ。

D. 考察

今回の CT 画像については、アンケート調査からの記述の検討である。いままでの報告と同様に、小葉間隔壁の肥厚や胸膜肥厚などの広義間質の病変の頻度が高かった。そのため、リンパ路にそった病変の進展が考えられた。

図2



患者1の肺組織像。胸膜・小葉間隔壁に沿った線維化・細胞浸潤

E. 結論

Erdheim-Chester 病の CT 画像所見として、小葉間隔壁の肥厚は特徴的であり、リンパ路にそった病変の進展が考えられた。

F. 研究発表

なし

G. 知的財産権の出願・登録状況

1. 特許取得

「該当なし」

2. 実用新案登録

「該当なし」

3. その他

「該当なし」

厚生労働省科学研究費補助金（難治性疾患等克服研究事業）
分担研究報告書

課題名

Erdheim-Chester 病に関する調査研究
(希少疾患領域の研究デザインに関する研究)

研究分担者：齋藤明子（独立行政法人国立病院機構 名古屋医療センター臨床研究センター
一臨床試験研究部 臨床疫学研究室）

研究要旨

Erdheim-Chester disease (ECD)は、非ランゲルハンス細胞性組織球症の一型で、全身に浸潤した組織球により骨痛、腎不全、心不全、肺線維症、尿崩症、眼球突出など多彩な症状を呈する疾患で、6割の患者が32ヶ月以内に死亡するとの予後不良な疾患である。世界的に見ても数百例程度の希少疾患であり、標準的治療法も改善されていないなど不明な点が多く存在する。本研究に関し、平成26年度は科横断的にECD症例情報を集積し、有病率、臨床症状、病変部位別の頻度等の基礎的なデータをまとめ、本邦におけるECD診療の実態を把握した。平成27年度は更に二次調査を行い、得られた詳細なデータより発症関連因子や予後関連因子などの解明を通じて重症度分類について検討した。今後、治療指針作成、ECD患者の診断及び治療の一助とすることが最終的な目標である。当研究室は、このような希少疾患による疾患の発生動向を確認する為の研究デザインの組み方、データ管理方法、統計解析手法などの方法論について担当した。

A. 研究目的

Erdheim-Chester disease (ECD)は、非ランゲルハンス細胞性組織球症の一型で、全身に浸潤した組織球により骨痛、腎不全、心不全、肺線維症、尿崩症、眼球突出など多彩な症状を呈する疾患で、6割の患者が32ヶ月以内に死亡するとの予後不良な疾患である。世界的に見ても数百例程度の希少疾患であり、標準的治療法も改善されていないなど不明な点が多く存在する。本研究に関し、平成26年度は科横断的にECD症例情報を集積し、有病率、臨床症状、病変部位別の頻度等の基礎的なデータをまとめ、平成27年度は協力が得られる施設より症例の二次調査にて詳細情報を取得し、本邦におけるECD診療の実態を把握した。さらに、

得られたデータより発症関連因子や予後関連因子などの解明を通じて重症度分類の確立、治療指針の作成を行い、ECD患者の診断及び治療の一助とすることが最終的な目標である。当研究室は、このような希少疾患による疾患の発生動向を確認する為の研究デザインの組み方、データ管理方法、統計解析手法などの方法論について担当した。

B. 研究方法

本研究は多施設共同後方視的調査研究として行う。希少疾患であることから、診療科横断的に幅広く一次調査を行い、日本国内におけるECD症例の概数を把握し、ECD症例が存在する施設に対し、詳細な臨床情報を得る目的で二次調査を行う方法を採用

用した。患者背景、家族歴、発症時期、診断時期、症状、浸潤臓器、合併症、血液検査所見、病理所見、これまでの治療内容と反応性、転帰等を調査項目とした。当研究室では、得られた情報を基に、国内における ECD 症例の患者背景など疫学的情報や予後因子などを研究事務局と共に検討する。

(倫理面への配慮)

研究は施設倫理委員会の承認の下に人権擁護上の配慮をもって行う。症例は、参加施設毎に匿名化番号が付与され、連結可能匿名化された番号を研究用に用いる。対応表は施設内で管理される。研究結果発表においても、被験者は特定されない形で学会や学術雑誌に公表する。

C. 研究結果

一次調査実施数に対する回答は、52%(2005/3850)であった。このうち、71例の ECD が同定され、二次調査として回収された 38 症例について、患者特性やアウトカムを分析した。

患者背景・疾患特性 (表 1)、治療内容 (表 2) について以下に示す。

表 1. 患者背景・疾患特性

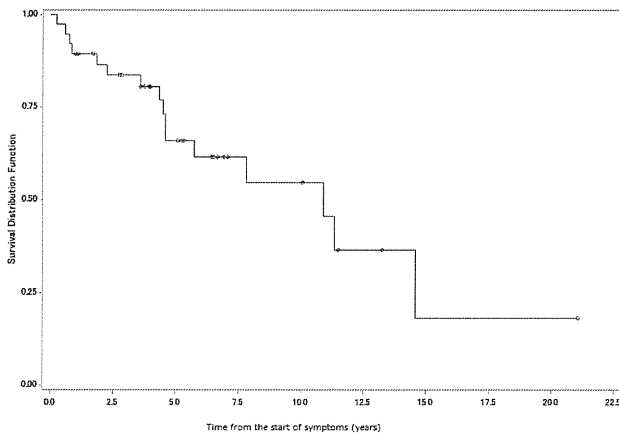
患者背景/疾患特性		n	%
性別			
	男	25	65.8
	女	13	34.2
初発時年齢 中央値 (範囲), 歳		51	(25-76)
診断時年齢 中央値 (範囲), 歳		54	(28-78)
診断年	1991-1999	5	13.2
	2000-2009	16	42.1
	2010-	17	44.7
初発から診断までの期間 中央値 (範囲), 月		17	(1-89)
発症からの観察期間 中央値 (範囲), 月		54	(3-253)
LCH既往		2	5.0
症状			
	全身症状	22	57.9
	発熱	14	36.8
	倦怠感	16	42.1
	体重減少	4	10.5
病変部位			
	複数病変	34	89.5
	骨病変	32	84.2
	中枢神経病変	20	52.6
	内分泌病変	16	42.1
	循環器病変	17	44.7
	呼吸器病変	11	29
	腎・後腹膜病変	17	44.7
	皮膚病変	16	42.1
	消化器病変	6	15.8
主病変	呼吸器	5	13.51
	骨	10	27.03
	循環器	4	10.81
	心臓	1	2.7
	腎後腹膜	2	5.41
	腎臓	2	5.41
	全身	1	2.7
	中枢神経	7	18.92
	内分泌	4	10.81
	皮膚	1	2.7

表 2. 治療内容

治療内容	n	%
IFN	10	26.3
ステロイド	22	57.9
放射線	5	13.2
保存的治療	30	79
支持療法(Bisphosphonate)	9	23.7
疼痛管理	7	18.4
その他	12	31.6

全 38 例の予後について、発症時からの生存時間解析結果を図 1 に示す。生存時間中央値は、10.9 年であった。

図 1. 全生存時間



Time(year)	Survivor Function	Std.Error
1	0.8947	0.0498
2	0.8659	0.0559
3	0.837	0.0611
4	0.806	0.0662
5	0.6595	0.0856

生命予後に影響を及ぼす因子について、Cox 解析を用いて探索した結果(単変量解析結果)を表 3 に示す。年齢が 60 歳以上の場合、ECD の浸潤臓器数が多い場合、骨病変が有る場合は、生命予後に負の影響を及ぼす(死亡リスクを上げる)可能性が示された。一方、体重減少、中枢神経病変、循環器病変、消化器病変はこの逆の所見が観察された。病変部位の重なりについて、図 2 の通りであった。表 3. 予後因子解析

予後因子		ハザード	Univariate analysis	
			95%信頼区間	P値
性別	vs. 女性	0.823	0.259-2.616	0.7400
年齢	vs. 60歳未満	26.888	5.337-135.446	<0.0001
臓器浸潤数	+1	1.488	1.073-2.063	0.0173
体重減少	vs. 無	0.193	0.051-0.735	0.0159
骨病変	vs. 無	4.899	1.590-15.096	0.0057
中枢神経病変	vs. 無	0.04	0.005-0.325	0.0026
内分泌病変	vs. 無	0.712	0.264-1.921	0.5020
循環器病変	vs. 無	0.293	0.099-0.874	0.0276
呼吸器病変	vs. 無	0.657	0.233-1.852	0.4268
腎・後腹膜病変	vs. 無	0.692	0.259-1.853	0.4644
皮膚病変	vs. 無	1.184	0.414-3.387	0.7527
消化器病変	vs. 無	0.185	0.052-0.664	0.0096

図 2 病変部位の重なり



D. 考察

回収された ECD 症例 38 例について、予備解析を行った。男性は女性の約 2 倍多く、診断時年齢中央値は 54 歳であった。複数病変を有する症例が多く、中でも骨病変を多く認めた。Median survival は約 10 年であり、高齢者、ECD の浸潤臓器数、骨病変の存在などが生命予後に負の影響を及ぼす可能性が示された。

E. 結論

希少な ECD の有病率、臨床症状、病変部位別頻度など基礎的データや診療実態を把握するため全国規模の調査を行い 38 例の収集された情報を用いた予備解析を実施した。症例数が少なく、断定的な結論は出せないため、症例集積を継続し、更なる分析を行う。

F. 研究発表

1. 論文発表
該当なし
2. 学会発表
該当なし

G. 知的財産権の出願・登録状況 (予定を含む。)

1. 特許取得
該当なし
2. 実用新案登録
該当なし
3. その他
該当なし

III. 研究成果の刊行に関する一覧

研究成果の刊行に関する一覧表

書籍

著者氏名	論文タイトル名	書籍全体の編集者名	書 籍 名	出版社名	出版地	出版年	ページ
村上有香子 片山一朗	組織球症. 幼少児によくみられる皮膚疾患アトラス-鑑別と治療のポイント	片山一朗 横関博雄	幼小児によくみられる皮膚疾患アトラス-鑑別と治療のポイント	医薬ジャーナル社	日本	2015	158-159

雑誌

発表者氏名	論文タイトル名	発表誌名	巻号	ページ	出版年
Yamamoto H, Lu J, Oba S, Kawamata T, Yoshimi A, Kurosaki N, Yokoyama K, Matsushita H, Kurokawa M, Tojo A, Ando K, Morishita K, Katagiri K, Kotani A.	miR-133 regulates Evi1 expression in AML cells as a potential therapeutic target.	Sci Rep.	12	19204.	2016
Kitamura K, Nishiyama T, Ishiyama K, Miyawaki S, Miyazaki K, Suzuki K, Masaie H, Okada M, Ogawa H, Imai K, Kiyoi H, Naoe T, Yokoyama Y, Chiba S, Hata T, Miyazaki Y, Hatta Y, Takeuchi J, Nannya Y, Kurokawa M, Ueda Y, Koga D, Sugiyama H, Takaku F.	Clinical usefulness of WT1 mRNA expression in bone marrow detected by a new WT1 mRNA assay kit for monitoring acute myeloid leukemia: a comparison with expression of WT1 mRNA in peripheral blood.	Int J Hematol.	103	53-62	2016
Morita K, Nakamura F, Taoka K, Satoh Y, Iizuka H, Masuda A, Seo S, Nannya Y, Yatomi Y, Kurokawa M.	Incidentally-detected t(9;22)(q34;q11)/BCR-ABL1-positive clone developing into chronic phase chronic myeloid leukaemia after four years of dormancy.	Br J Haematol.	In press		2015

Wong WF, Kohu K, Nagashima T, Funayama R, Matsumoto M, Movahed E, Tan GM, Yeow TC, Looi CY, Kurokawa M, Osato M, Igarashi K, Nakayama K, Satake M.	The artificial loss of Runx1 reduces the expression of quiescence-associated transcription factors in CD4(+) T lymphocytes.	Mol Immunol.	68	223-233.	2015
Shibata S, Tada Y, Hau CS, Mitsui A, Kamata M, Asano Y, Sugaya M, Kadono T, Masamoto Y, Kurokawa M, Yamauchi T, Kubota N, Kadowaki T, Sato S.	Adiponectin regulates psoriasisiform skin inflammation by suppressing IL-17 production from $\gamma\delta$ -T cells.	Nat Commun.	15	7687	2015
Arai S, Miyauchi M, Kurokawa M.	Modeling of hematologic malignancies by iPS technology.	Exp Hematol.	43	654-660	2015
Iizuka H, Kagoya Y, Kataoka K, Yoshimi A, Miyauchi M, Taoka K, Kumano K, Yamamoto T, Hotta A, Arai S, Kurokawa M.	Targeted gene correction of RUNX1 in induced pluripotent stem cells derived from familial platelet disorder with propensity to myeloid malignancy restores normal megakaryopoiesis.	Exp Hematol.	43	849-857	2015
Kobayashi H, Kobayashi CI, Nakamura-Ishizu A, Karigane D, Haeno H, Yamamoto KN, Sato T, Ohteki T, Hayakawa Y, Barber GN, Kurokawa M, Suda T, Takubo K.	Bacterial c-di-GMP affects hematopoietic stem/progenitors and their niches through STING.	Cell Rep.	11	71-84	2015
Hirokawa M, Sawada K, Fujishima N, Teramura M, Bessho M, Dan K, Tsurumi H, Nakao S, Urabe A, Fujisawa S, Yonemura Y, Kawano F, Oshimi K, Sugimoto K, Matsuda A, Karasawa M, Arai A, Komatsu N, Harigae H, Omine M, Ozawa K, Kurokawa M	PRCA Collaborative Study Group. Long-term outcome of patients with acquired chronic pure red cell aplasia (PRCA) following immunosuppressive therapy: a final report of the nationwide cohort study in 2004/2006 by the Japan PRCA collaborative study group.	Br J Haematol.	169	879-886	2015

IV. 研究成果の刊行物・別刷

(主なもの)

Incidentally-detected t(9;22)(q34;q11)/BCR-ABL1- positive clone developing into chronic phase chronic myeloid leukaemia after four years of dormancy

The World Health Organization (WHO) Classification (4th Edition) assigns chronic myeloid leukaemia (CML) to the myeloproliferative neoplasms, which are defined as clonal disorders with proliferation of one or more of the myeloid lineages. CML is characterized by t(9;22)(q34;q11) translocation and resultant *BCR-ABL1* fusion gene found in all myeloid lineages as well as lymphoid cells and endothelial cells. We herein describe a case of incidentally-detected t(9;22)(q34;q11)/*BCR-ABL1*-positive clones developing into CML after a dormancy period. Our case highlights the significance of distinction between subclinical and definite CML.

A 64-year-old woman was referred to us for systemic evaluation of refractory primary intraocular lymphoma (PIOL). She had received topical therapy with intravitreal methotrexate injections for the preceding 4 months. Imaging studies did not find any intracranial or distant lesions. The bone marrow (BM) was unremarkable without lymphoma infiltration (Fig 1A). Of note, routine G-banded karyotyping identified t(9;22)(q34;q11) in five of 20 metaphase cells analysed (Fig 1B). We considered the possibility of CML; however, the BM was normocellular without increase in neutrophils or neutrophil precursors. The myeloid:erythroid ratio was within a normal range and no fibrosis was detected. Thus, the BM lacked morphological features of CML. The patient did not complain of fatigue or weight loss and there was no evidence of splenomegaly. Laboratory findings were unremarkable, including white blood cell (WBC) count of $5.6 \times 10^9/l$ with normal differential, haemoglobin level 126 g/l, and platelet count $274 \times 10^9/l$. Reverse transcription-nested polymerase chain reaction (RT-nested PCR) assay of peripheral blood (PB) detected e14/a2 (b3/a2) *BCR-ABL1* mRNA. Real-time PCR using the LightCycler[®] system (Roche Diagnostics, Mannheim, Germany) revealed *BCR-ABL1* level (normalized to *RNA18S1*) of 4.00×10^{-5} . Regular fluorescence *in situ* hybridization (FISH) analysis for t(9;22)(q34;q11)/*BCR-ABL1* using LSI-BCR/ABL dual colour ES probe (Vysis Inc., Downers Grove, IL, USA) did not detect *BCR-ABL1* fusion signals either in BM mononuclear cells or in PB neutrophils. We then performed metaphase FISH analysis on BM, which revealed fusion signals in 13 (33%) of 40 metaphases scored. Thus, the discrepancy between the findings of G-banding and interphase FISH analysis was explained by the growth difference between the t(9;22)(q34;q11)/*BCR-*

ABL1-positive cells and normal haematopoietic precursors in the *ex vivo* culture system. Despite positive cytogenetic and molecular findings, lack of myeloid lineage proliferation hampered the diagnosis of CML. Thus, systemic treatment for PIOL, comprising chemoimmunotherapy and whole brain radiotherapy was prioritized according to the protocol at our institution (Taoka *et al*, 2012). *BCR-ABL1* mRNA was negative upon completion of the treatment (Fig 2). We employed a watchful waiting strategy for the t(9;22)(q34;q11)/*BCR-ABL1*-positive clones by monitoring *BCR-ABL1* level using real-time PCR as previously described (Emig *et al*, 1999). RT-nested PCR for *BCR-ABL1* mRNA became positive in six months and the *BCR-ABL1* level gradually increased during the following three years. FISH analyses for t(9;22)(q34;q11) in PB neutrophils were repeatedly negative. *BCR-ABL1* level eventually reached 2.78×10^{-1} , which was almost comparable to the mean level (5.87×10^{-1}) of 30 newly diagnosed CML patients at our institution (Nannya *et al*, 2008). Laboratory results showed a slightly increased WBC count of $9.8 \times 10^9/l$ with mild basophilia. The patient remained asymptomatic and without splenomegaly. A follow-up BM analysis showed a hypercellular marrow with proliferation of myeloid lineage cells (Fig 1C). G-banded karyotyping identified t(9;22)(q34;q11) in 17 of 20 metaphases, and FISH analysis of BM aspirate detected *BCR-ABL1* fusion signals in 82% of interphase cells scored. The fusion signals were also present in 94% of PB neutrophils and 20% of PB mononuclear cells (Fig 1D). These findings confirmed the diagnosis of chronic phase CML, and treatment was initiated with dasatinib. After three months, G-banding and FISH analyses of BM indicated a normal karyotype, and real-time PCR analysis showed a 3.5-log decrease in PB *BCR-ABL1* level.

Incidentally-detected t(9;22)/*BCR-ABL1*-positive clones failing to meet the criteria for CML may be considered as subclinical CML, which can progress to definitive CML after a dormant period. Subclinical CML can be morphologically distinguished from definitive CML in that it lacks proliferation of myeloid lineages. Subclinical CML is therefore not classified as CML or even as a myeloproliferative neoplasm according to the WHO classification. In our case, previous intravitreal methotrexate injection therapy was probably irrelevant to the pathogenesis of subclinical CML, considering its

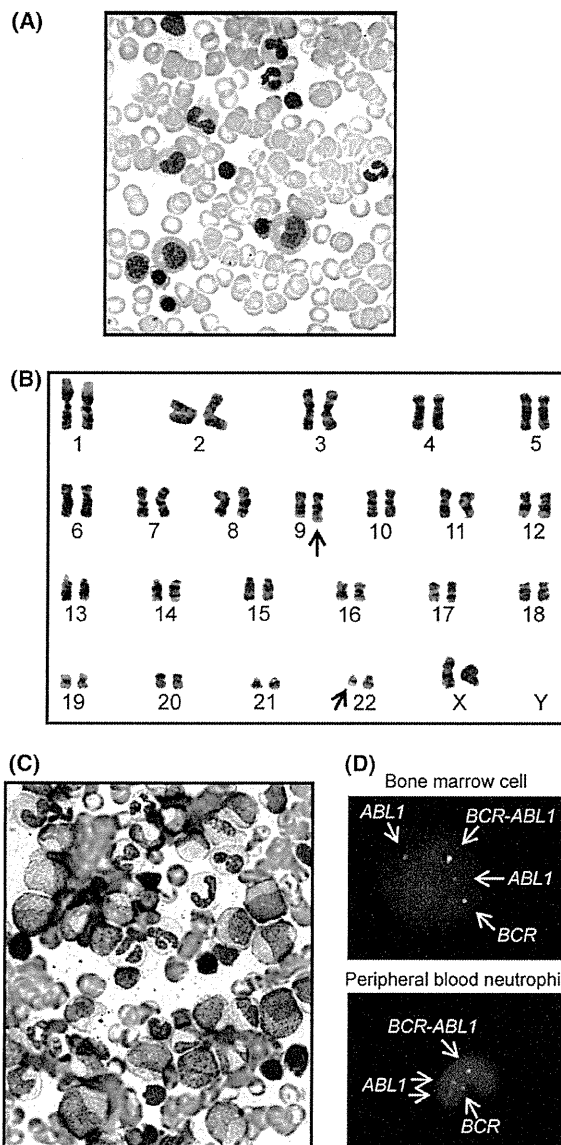


Fig 1. Bone marrow morphology and cytogenetic findings at initial detection of the t(9;22)(q34;q11) translocation and upon progression to definite chronic myeloid leukaemia. (A) Bone marrow analysis at initial detection showed a normocellular marrow without infiltration of lymphoma cells. There were no morphological features of CML. (B) G-banding of bone marrow aspirate at initial detection unexpectedly showed the t(9;22)(q34;q11) translocation (arrows). (C) Bone marrow analysis upon progression to definite CML revealed a markedly hypercellular marrow with proliferation of myeloid lineage cells. (D) FISH analysis upon progression to definite CML detected *BCR-ABL1* fusion signals in a bone marrow mononuclear cell (upper panel) and a peripheral blood neutrophil (lower panel). We used the LSI-*BCR/ABL* dual colour ES probe, which produces green *BCR* signals and red *ABL1* signals. Note that the *ABL1* probe covers the breakpoint, yielding an extra *ABL1* signal.

topical nature and an extremely short latency. On the other hand, systemic treatment for PIOL, particularly radiotherapy, may have contributed to the transition from subclinical to

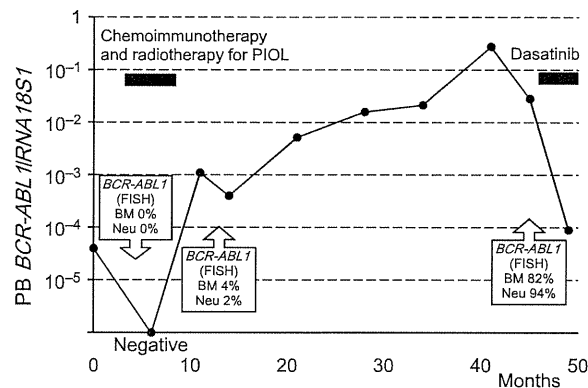


Fig 2. Clinical course of our patient with an incidentally detected t(9;22)/*BCR-ABL1*-positive clone. *BCR-ABL1* mRNA expression in peripheral blood was monitored following the initial detection of a cytogenetic abnormality. *BCR-ABL1* fusion transcripts were quantified by real-time PCR using LightCycler® system (Roche Diagnostics). Levels of *BCR-ABL1* mRNA were normalized to those of *RNA18S1*, which served as an internal control. PIOL, primary intraocular lymphoma; FISH, fluorescence *in situ* hybridization; BM, bone marrow; Neu, neutrophils.

definite CML; exposure to ionizing radiations is a well-known cause of CML (Bizzozero *et al*, 1966).

Coexistence of subclinical CML and another haematological disease is a rare but recurrent event. Two such cases have been reported thus far. One case was a 74-year-old man with monoclonal gammopathy (Shani & Malik, 2009), and the other was a 60-year-old man with multiple myeloma after autologous haematopoietic stem cell transplant (Roper *et al*, 2010). In both cases, G-banded karyotyping and FISH analysis unexpectedly detected t(9;22)(q34;q11)/*BCR-ABL1*-positive clones, whilst proliferation of the myeloid lineages was absent. Treatment with imatinib for subclinical CML was commenced immediately and eight weeks after the initial t(9;22)(q34;q11) detection, respectively.

A treatment strategy for subclinical CML has not been established. There is no evidence to demonstrate the advantage of early intervention over watchful waiting, especially considering the possible adverse effects associated with tyrosine kinase inhibitors (Gunnarsson *et al*, 2015). No data are available regarding spontaneous regression or long-term treatment outcomes of subclinical CML due to the rarity of such condition. However, the excellent efficacy of tyrosine kinase inhibitors for definite chronic phase CML confers a relatively low risk to watchful waiting strategy. Comprehensively, we decided to adopt watchful waiting strategy in our case.

BCR-ABL1 mRNA is detected in a substantial portion of healthy individuals. A study using the semi-nested PCR technique revealed that *BCR-ABL1* (p210) transcript was positive in 30% of healthy adults and 5% of healthy children (Biernaux *et al*, 1995). The mere positivity of *BCR-ABL1* mRNA without cytogenetic abnormalities is not therefore clinically

significant when we consider the prevalence of CML. Nevertheless, our case teaches us that the *BCR-ABL1*-positive population may also have a propensity to develop definite CML after radiotherapy and/or chemoimmunotherapy.

Acknowledgments

The authors appreciate Ms. Yoko Hokama for performing sequencing analysis.

Author contributions

KM and FN designed the study. FN, YS, KT, AM, SS and HI provided important clinical data. KM, FN and MK wrote the paper. AM, YN, YY and KM critically revised the manuscript. MK supervised the entire work. All authors approved the final manuscript.

Conflict of interest

This is not a sponsored study, but we declare the potential conflict of interest with the pharmaceutical companies that deal with the drugs described in this study. KM was temporarily employed as Scientific Summer Intern by PRO Unlimited onsite working at Novartis Institutes for BioMedical Research; FN received speaking fee from Novartis Pharma Japan Inc.; KT, YS, HI, AM and YY report no conflict of interest; SS received speaking fee from Bristol-Myers Squibb

Company; YN received grant from Pfizer Japan Inc., speaking fee from Novartis Pharma Japan Inc and Bristol-Myers Squibb Company, and served as a member of advisory board of Bristol-Myers Squibb; MK received grant from Pfizer Japan Inc., grant and speaking fee from Novartis Pharma Japan Inc and Bristol-Myers Squibb Company. MK also reports that he was a member of the technical advisory board of Novartis Pharma Japan Inc and Bristol-Myers Squibb.

Kiyomi Morita¹
Fumihiko Nakamura¹
Kazuki Taoka¹
Yumiko Satoh²
Hiromitsu Iizuka¹
Akiko Masuda²
Sachiko Seo¹
Yasuhito Nannya¹
Yutaka Yatomi²
Mineo Kurokawa¹

¹Department of Haematology and Oncology, Graduate School of Medicine, The University of Tokyo, and ²Department of Clinical Laboratory Medicine, The University of Tokyo Hospital, Tokyo, Japan
E-mail: kurokawa-ky@umin.ac.jp

Keywords: *BCR-ABL1*, chemoimmunotherapy, chronic myeloid leukaemia, radiotherapy, subclinal

References

- Biernaux, C., Loos, M., Sels, A., Huez, G. & Stryckmans, P. (1995) Detection of major bcr-abl gene expression at a very low level in blood cells of some healthy individuals. *Blood*, **86**, 3118–3122.
- Bizzozero, O.J., Johnson, K.G. & Ciocco, A. (1966) Radiation-related leukemia in Hiroshima and Nagasaki, 1946–1964. I. Distribution, incidence and appearance time. *New England Journal of Medicine*, **274**, 1095–1101.
- Emig, M., Saussele, S., Wittor, H., Weisser, A., Reiter, A., Willer, A., Berger, U., Hehlmann, R., Cross, N.C. & Hochhaus, A. (1999) Accurate and rapid analysis of residual disease in patients with CML using specific fluorescent hybridization probes for real time quantitative RT-PCR. *Leukemia*, **13**, 1825–1832.
- Gunnarsson, N., Stenke, L., Höglund, M., Sandin, F., Björkholm, M., Dreimane, A., Lambe, M., Markevårn, B., Olsson-Strömberg, U., Richter, J., Wadenvik, H., Wallvik, J. & Sjölander, A. (2015) Second malignancies following treatment of chronic myeloid leukaemia in the tyrosine kinase inhibitor era. *British Journal of Haematology*, **169**, 683–688.
- Nannya, Y., Yokota, H., Sato, Y., Yamamoto, G., Asai, T., Ichikawa, M., Watanabe, T., Kumano, K., Hangaishi, A., Takahashi, T., Chiba, S., Yatomi, Y. & Kurokawa, M. (2008) Molecular and cytogenetic response of chronic myelogenous leukemia treated with imatinib mesylate: one institutional experience in Japan. *International Journal of Hematology*, **88**, 159–164.
- Roper, N., DeAngelo, D.J., Kuo, F., Dal Cin, P., Ghobrial, I. & Aster, J.C. (2010) An asymptomatic 61-year-old man with BCR-ABL-positive bone marrow following autologous transplantation for multiple myeloma. *American Journal of Hematology*, **85**, 944–946.
- Shani, D. & Malik, A. (2009) Incidental diagnosis of CML in a patient with anemia and IgG lambda monoclonal protein in blood. *Annals of Hematology*, **88**, 1041.
- Taoka, K., Yamamoto, G., Kaburaki, T., Takahashi, T., Araie, M. & Kurokawa, M. (2012) Treatment of primary intraocular lymphoma with rituximab, high dose methotrexate, procarbazine, and vincristine chemotherapy, reduced whole-brain radiotherapy, and local ocular therapy. *British Journal of Haematology*, **157**, 252–254.

ARTICLE

Received 23 Mar 2015 | Accepted 2 Jun 2015 | Published 15 Jul 2015

DOI: 10.1038/ncomms8687

Adiponectin regulates psoriasiform skin inflammation by suppressing IL-17 production from $\gamma\delta$ -T cells

Sayaka Shibata¹, Yayoi Tada^{1,2}, Carren Sy Hau², Aya Mitsui¹, Masahiro Kamata¹, Yoshihide Asano¹, Makoto Sugaya¹, Takafumi Kadono¹, Yosuke Masamoto³, Mineo Kurokawa³, Toshimasa Yamauchi⁴, Naoto Kubota⁴, Takashi Kadowaki⁴ & Shinichi Sato¹

Accumulating epidemiologic evidence has revealed that metabolic syndrome is an independent risk factor for psoriasis development and is associated with more severe psoriasis. Adiponectin, primarily recognized as a metabolic mediator of insulin sensitivity, has been newly drawing attention as a mediator of immune responses. Here we demonstrate that adiponectin regulates skin inflammation, especially IL-17-related psoriasiform dermatitis. Mice with adiponectin deficiency show severe psoriasiform skin inflammation with enhanced infiltration of IL-17-producing dermal V γ 4 + $\gamma\delta$ -T cells. Adiponectin directly acts on murine dermal $\gamma\delta$ -T cells to suppress IL-17 synthesis via AdipoR1. We furthermore demonstrate here that the adiponectin level of skin tissue as well as subcutaneous fat is decreased in psoriasis patients. IL-17 production from human CD4- or CD8-positive T cells is also suppressed by adiponectin. Our data provide a regulatory role of adiponectin in skin inflammation, which would imply a mechanism underlying the relationship between psoriasis and metabolic disorders.

¹Department of Dermatology, University of Tokyo Graduate School of Medicine, 7-3-1 Hongo, Bunkyo-ku, Tokyo 113-8655, Japan. ²Department of Dermatology, Teikyo University School of Medicine, 2-11-1 Kaga, Itabashi-ku, Tokyo 173-8605, Japan. ³Department of Hematology and Oncology, University of Tokyo Graduate School of Medicine, 7-3-1 Hongo, Bunkyo-ku, Tokyo 113-8655, Japan. ⁴Department of Diabetes and Metabolic Diseases, University of Tokyo Graduate School of Medicine, 7-3-1 Hongo, Bunkyo-ku, Tokyo 113-8655, Japan. Correspondence and requests for materials should be addressed to Y.T. (email: ytada-tky@umin.ac.jp).

Psoriasis is a common chronic inflammatory skin disease, affecting ~2–3% of the world's population, which is characterized by epidermal hyperplasia, inflammatory cell infiltration and vascular changes^{1,2}. In the development of psoriasis, keratinocytes and immune cells interact with each other through the production of cytokines. This cellular interplay, especially via the interleukin (IL)-23/Th17 cytokine network, finally leads to psoriatic plaque formation. IL-23, secreted by dendritic cells, differentiates naive T cells into Th17 cells, and these activated Th17 cells further secrete IL-17A, IL-17F and IL-22, which finally cause keratinocyte proliferation^{3–5}. The importance of the IL-23/Th17 axis has been also exemplified by the therapeutic efficacy of human monoclonal antibodies targeting IL-12/23p40 (ustekinumab), IL-17 (ixekizumab and secukinumab) and its receptor (brodalumab)^{6–8}.

Psoriasis has been long considered to be a skin-tropic and not life-threatening disease; however, it is now increasingly recognized that psoriasis inflammation is not limited to the skin but goes far beyond the skin, accompanying systemic inflammation^{9,10}. Immune cells and cytokines, when released into the systemic circulation, may alter the function of endothelial and haematopoietic cells, leading to the increase in the risk of insulin resistance and atherosclerosis. This inflammatory cascade is named 'psoriatic march', and psoriasis patients are now considered to be at higher risk of developing metabolic syndrome¹¹. Systemic inflammation induced by obesity and metabolic syndrome, in turn, could exacerbate local skin inflammation via blood flow, which may consequently expand psoriasis inflammation¹². The link between local and systemic inflammation is further supported by recent vast reports focusing on the high percentages of psoriasis patients who have cardiovascular and metabolic comorbidities^{12–17}.

Adipose tissue, although considered as an organ for energy storage in the past, is now accepted as an active endocrine and immune organ, which produces various bioactive molecules, named adipokines^{18,19}. These adipokines, in cooperation with macrophages and T cells, cause adipose tissue inflammation and finally develop metabolic syndrome. Among these adipokines, adiponectin is a representative and main mediator of metabolism^{20,21}. Interestingly, recent reports regarding adiponectin have been focusing on a new feature of adiponectin, an aspect as a regulator of immune responses^{22,23}. A number of experimental studies suggest that adiponectin attenuates excessive inflammatory responses in a variety of tissues, especially in obesity-associated states^{24–26}. Roles of adiponectin in the development of psoriasis, one of the obesity-linked diseases as mentioned above, have been also discussed in the vast past epidemiologic reports^{27–29}. Serum adiponectin levels are decreased in psoriasis patients compared with healthy controls and its levels increase along with the improvement of dermatitis after successful treatments, including anti-tumour necrosis factor (TNF)- α agents, suggesting that adiponectin negatively regulates psoriasis progression^{30,31}. Adiponectin *in vitro* suppresses TNF- α , IL-6 and IL-12p40 production from THP-1 cells, and IL-6 production from normal human keratinocytes³⁰. These results have led us to further investigate whether adiponectin actually influences psoriasis inflammation *in vivo*.

In the past few years, a mouse model of psoriasiform dermatitis induced by topical imiquimod application, has been frequently used to examine the inflammatory responses of the skin^{32,33}. In this model, mice are treated topically with imiquimod cream for 6 consecutive days. After 6 days, rapid inflammation is noted in murine skin that resembles the clinical manifestation and histopathology of human psoriasis. In addition, this model mirrors the cytokine profile of human psoriasis, especially that of

the IL-23/Th17-related pathway. Although this model indeed demonstrates a simple and acute skin inflammation and is not sufficient to replicate a chronic and complex human condition, alongside human studies, this model would be provided as one of the established ways to understand the immunological aspects of human disease³⁴. The purpose of this study is to elucidate the possible roles of adiponectin in the development of psoriasis, using imiquimod- and IL-23-induced murine models of psoriasiform dermatitis along with human samples. We show here that lack of adiponectin exacerbates psoriasis-like skin inflammation with excessive infiltration of IL-17-producing V γ 4+ dermal $\gamma\delta$ -T cells. Furthermore, adiponectin directly acts on dermal $\gamma\delta$ -T cells to suppress IL-17 production. These results are in agreement with human data displaying the decreased level of adiponectin in subcutaneous fat and skin tissue of psoriasis patients. We also demonstrate regulatory roles of adiponectin on human CD4- and CD8-positive T cells. Although numerous reports have reported anti-inflammatory aspects of adiponectin on a variety of cell types, our data provides new evidence that adiponectin also has an anti-inflammatory effect on T cells and regulates skin inflammation.

Results

Adiponectin deficiency exacerbates psoriasiform dermatitis. To examine the role of endogenous adiponectin during psoriasiform skin inflammation *in vivo*, we first applied imiquimod cream on mouse back skin, and investigated the clinical and histopathological features of wild-type and adiponectin-deficient mice. We also applied imiquimod cream on mouse ear skin and evaluated ear thickness. We confirmed that there are no differences in the phenotype or cytokine expressions between mice applied with Vaseline and a cream containing isostearic acid (25% w/w), a major component of the vehicle cream of the imiquimod (Supplementary Fig. 1). Thus, we used Vaseline as a control cream of imiquimod in this study. Adiponectin-deficient mice exhibited worse clinical outcome with more severe scales and thicker skin at day 4–6 of imiquimod treatment as compared with wild-type mice (Fig. 1a). Clinical scores for disease severity were calculated daily using a scoring system based on the clinical Psoriasis Area and Severity Index. Significant differences in disease severity and ear thickness were observed between wild-type and adiponectin-deficient mice from day 4 to 6 (Fig. 1b). Consistent with clinical scores, histological analyses of skin samples at day 5 of imiquimod treatment on mouse back skin showed more severe epidermal hyperplasia and more intense inflammatory cell infiltration in adiponectin-deficient mice as compared with wild-type mice (Fig. 1c). Immunohistochemistry analyses revealed that infiltrating cells in the upper dermis were CD3 or major histocompatibility complex class II positive, and that cell counts for these positive cells were significantly increased in adiponectin-deficient mice compared with wild-type mice (Fig. 1d).

Adiponectin deficiency promotes IL-17A gene expression. We next examined the messenger RNA (mRNA) expression levels of psoriasis-related cytokines in the imiquimod-induced psoriasiform skin lesions of wild-type and adiponectin-deficient mice. Skin samples were taken from mouse back skin, before treatment, and 24 or 48 h after imiquimod application. Messenger RNA levels for TNF- α , IFN- γ , IL-6, IL-12p40, IL-23p19, IL-17A, IL-17F and IL-22 were determined by quantitative real-time PCR. Imiquimod-treated skin demonstrated increased mRNA levels of genes mentioned above, and adiponectin deficiency further augmented mRNA levels of TNF- α , IL-6, IL-12p40 and IL-23p19, which would reflect the anti-inflammatory roles of adiponectin

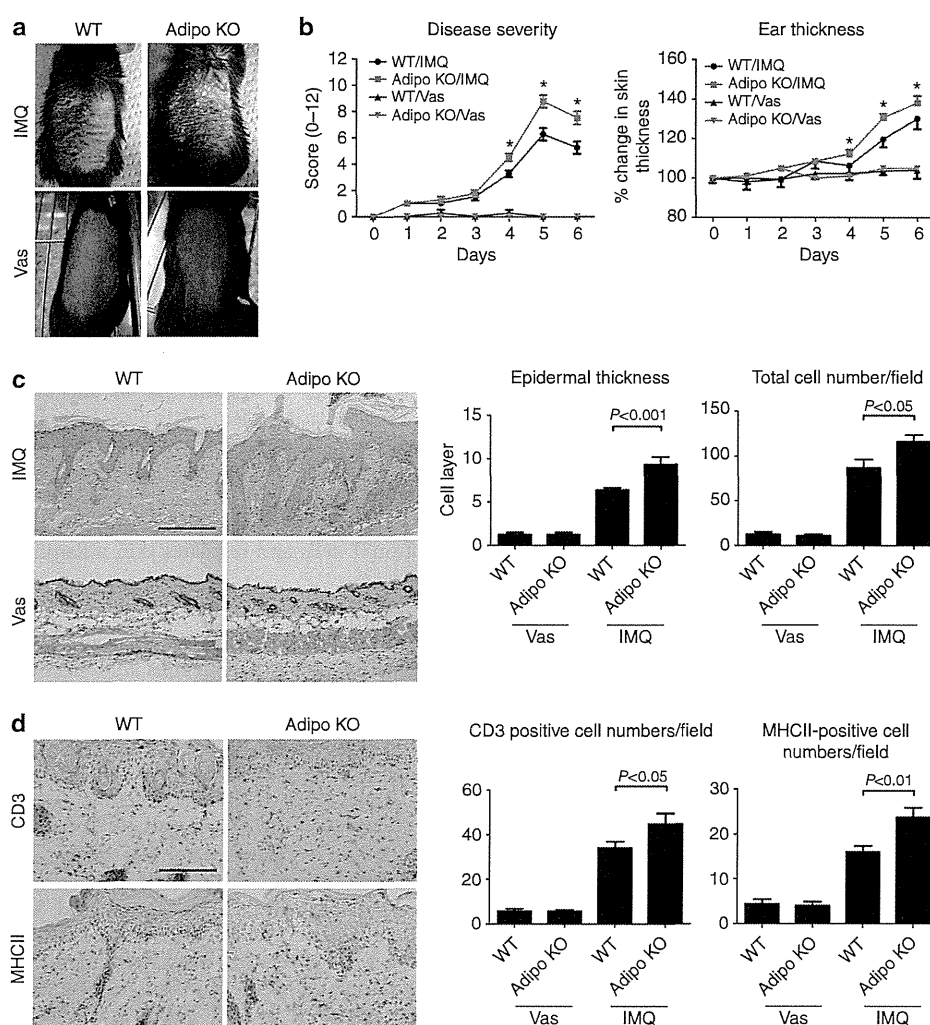


Figure 1 | Adiponectin deficiency promotes psoriasisform dermatitis. Shaved back skin and ears of wild-type (WT) and adiponectin-deficient (Adipo knockout (Adipo KO)) mice were topically treated with imiquimod (IMQ) or control Vaseline (Vas) for 6 consecutive days. **(a)** Phenotypic manifestation of WT and Adipo KO mouse back skin induced by IMQ or Ctrl cream application at day 5. **(b)** Disease severity (left panel) and ear thickness (right panel) during IMQ or Vas treatment. Clinical scores for disease severity were calculated daily using a scoring system based on the clinical Psoriasis Area and Severity Index. Data are presented as mean \pm s.e. ($n = 3-5$ for each group). * $P < 0.05$ versus WT mice with IMQ application. **(c)** Histological presentation of WT and Adipo KO mouse back skin induced by IMQ or Vas application at day 5 ($\times 200$). Scale bar, 50 μm . The number of epidermal cell layers and dermal inflammatory cells was counted per high-power field from 3 to 5 mice per group. Data are presented as mean \pm s.e. ($n = 3-5$). **(d)** Immunohistochemical presentation of WT and Adipo KO mouse back skin induced by IMQ or Vas application at day 5 ($\times 400$). Scale bar, 25 μm . The number of CD3 or major histocompatibility complex (MHC) class II (MHCII)-positive cells was counted per high-power field from 3 to 5 mice per group. Data are presented as mean \pm s.e. ($n = 3-5$), and analysed by Welch's *t*-test for **b-d**.

on macrophages and dendritic cells. In addition, mRNA levels of IL-17A, IL-17F and IL-22 were also markedly upregulated in adiponectin-deficient mice at 48 h after imiquimod application, as compared with wild-type mice (Fig. 2a). In the experiment of intradermal IL-23 injections to mouse ear skin, another widely used model of psoriasisform skin inflammation, IL-17A/IL-17F/IL-22 expression was upregulated after IL-23 injection^{33,35}, and adiponectin deficiency further increased their expression level (Fig. 2b). Interestingly, IL-17A expression was much greater with IL-23 injection than imiquimod treatment, whereas IL-17F and IL-22 were far less responsive to IL-23 injection than to imiquimod treatment in adiponectin-deficient mice, suggesting that the major effect of adiponectin is on IL-17A. Thus, we sought to focus on the effect of adiponectin especially on IL-17A. Notably, there was great increase in both IL-6 and IL-17A

expression in adiponectin-deficient mice at 48 h after imiquimod application (Fig. 2a). In detail, IL-6 was sufficiently produced after 24 h of imiquimod application, whereas IL-17A was gradually produced until 48 h in adiponectin-deficient mice, suggesting the possibility that IL-6 overproduction in adiponectin-deficient mice might predominate further increase in IL-17A production at 48 h. To address this concern, we conducted an intraperitoneal injection of IL-6 antibody in both adiponectin-deficient and wild-type mice, and then compared IL-17A expression level 48 h after imiquimod application. As shown in Fig. 2c, IL-6 antibody injection suppressed, but not significantly, about half of IL-17A production in wild-type mice. In adiponectin-deficient mice, suppression level of IL-17A by IL-6 antibody was more remarkable as compared with that in wild-type mice. This result would imply that the IL-17A production

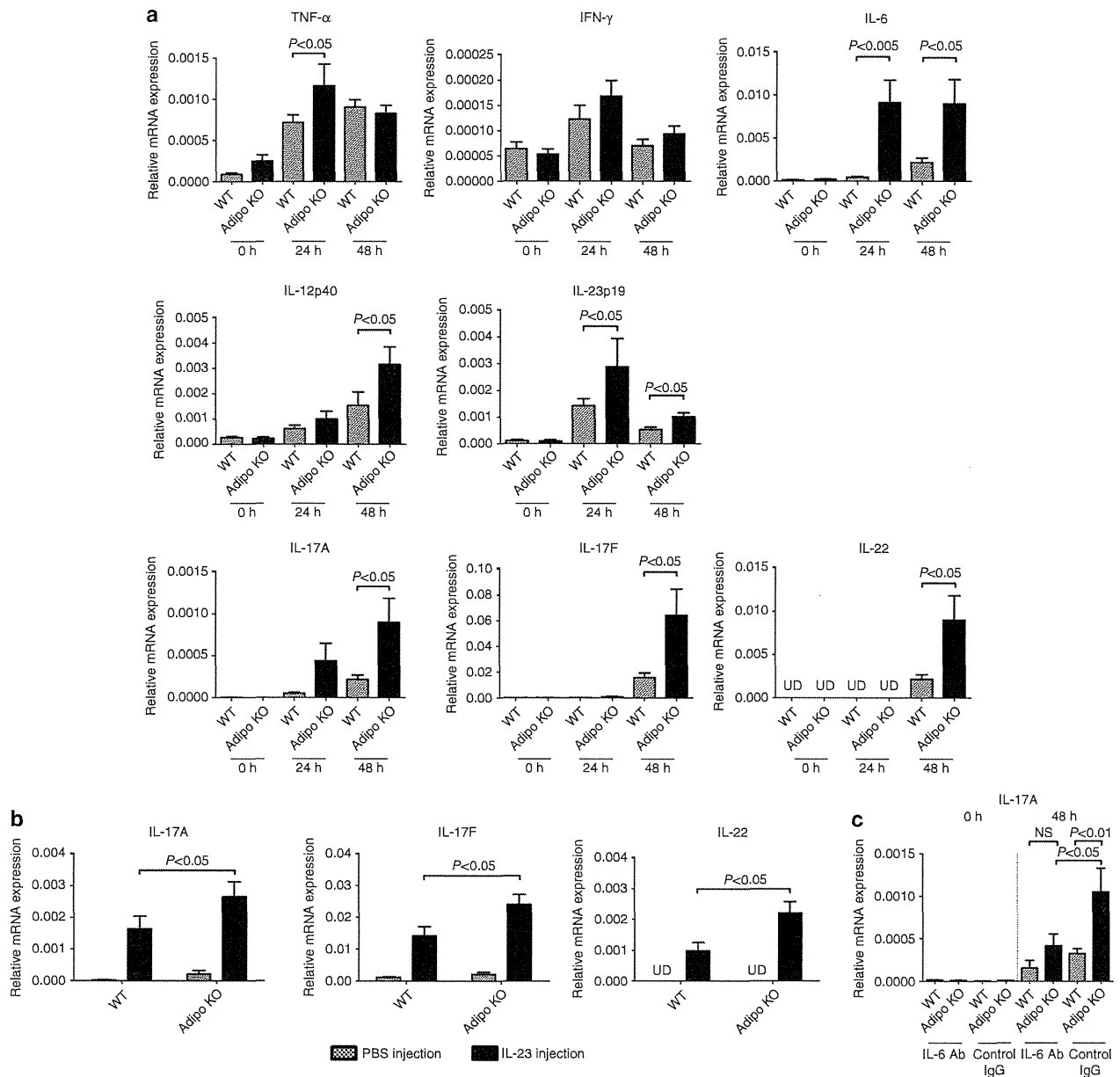


Figure 2 | Adiponectin deficiency promotes gene expression of cytokines implicated in the psoriasisform skin inflammation. Wild-type (WT) and Adiponectin knockout (Adipo KO) mice were (a) applied with imiquimod (IMQ) or (b) injected with IL-23 intradermally, and skin samples were taken (a) before treatment, and 24 or 48 h after IMQ application or (b) after second IL-23 injection. Messenger RNA levels of the indicated cytokines were determined by quantitative PCR. Data are obtained from duplicate samples from 5 to 8 mice in each group. Values are presented as mean \pm s.e. ($n = 10-16$). UD, undetected. (c) WT and Adipo KO mice were injected with IL-6 antibody intraperitoneally, and IL-17A mRNA level of skin samples was determined before treatment and 48 h after IMQ application. Data are obtained from duplicate samples from 2 to 4 mice in each group. Values are presented as mean \pm s.e. ($n = 4$; 0 h, $n = 8$; 48 h). Data are analysed by Welch's *t*-test for a,b and by one-way analysis of variance with Dunnett's multiple comparison test for c. NS, not significant.

might be regulated partially by IL-6 in the imiquimod-induced skin inflammation and that the enhanced IL-6 production by adiponectin deficiency might induce subsequent IL-17A production and exacerbation of dermatitis.

Adiponectin regulates IL-17A-producing dermal $\gamma\delta$ -T cells. To clarify whether adiponectin deficiency is actually involved in the local skin inflammation, we next performed intracellular flow cytometric analyses of the skin after imiquimod application.

Single-cell suspensions from the dermis separated from the epidermis of wild-type and adiponectin-deficient mice after 5 days of imiquimod treatment were stimulated with phorbol 12-myristate 13-acetate (PMA) and ionomycin, and then were analysed for IL-17A as well as CD3 and $\gamma\delta$ TCR expression. Adiponectin deficiency promoted the recruitment of CD3-positive cells to the dermis of imiquimod-induced skin as compared with wild-type mice (Fig. 3a,b). The proportion of $\gamma\delta$ -T cells among these infiltrating CD3-positive cells was similar between wild-type and adiponectin-deficient mice (Fig. 3c,d). In addition, as well as

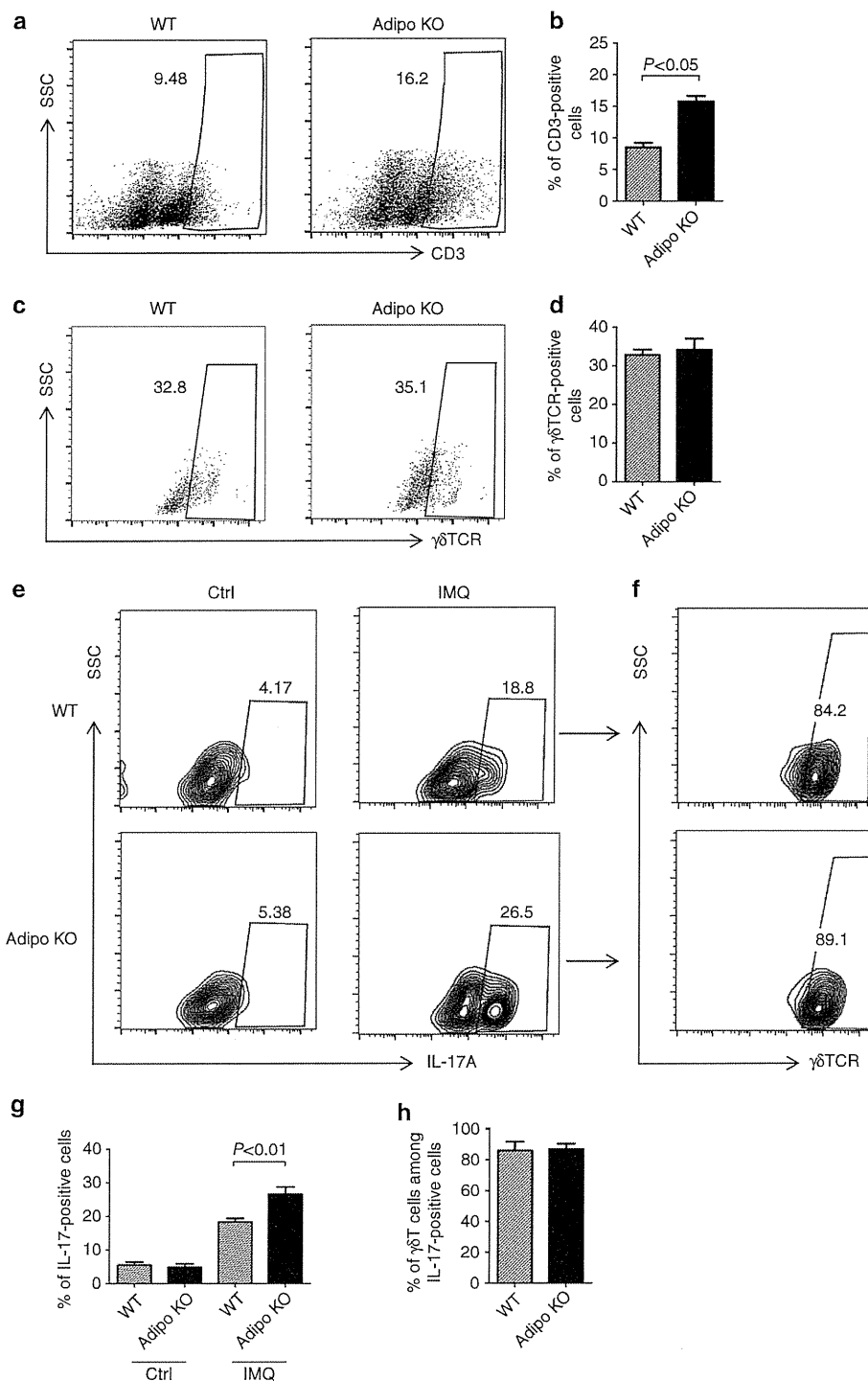


Figure 3 | Adiponectin negatively regulates the recruitment of inflammatory cells and the IL-17 production from $\gamma\delta$ -T cells in the skin. Wild-type (WT) and Adiponectin knockout (Adipo KO) mice were treated as described. At day 5, dermal cell suspensions of mouse back skin were stimulated with PMA and ionomycin, and were stained with antibodies specific for IL-17A as well as CD3 and TCR $\gamma\delta$ cell surface markers, followed by flow cytometric analysis. Gating strategy is shown in Supplementary Fig. 3. **(a,c,e,f)** Flow plots show the CD3-positive **(a)**, TCR $\gamma\delta$ -positive **(c,f)**, IL-17A-positive **(e)** population of the dermal cells from WT and Adipo KO mice. Flow plots were gated on CD3-positive cells **(c,e)**. **(b,d,g,h)** Graph shows the percentage of CD3-positive **(b)**, TCR $\gamma\delta$ -positive **(d,h)** and IL-17-positive **(g)** cells. The percentage of IL-17-positive cells among CD3 cells of each group is shown in Supplementary Table 1. Values are presented as mean \pm s.e. ($n = 6$). Data are representative of three independent experiments, where each group contains 1 to 2 mice. Data are analysed by Welch's *t*-test for **a,b,g,h**. IMQ, imiquimod.

increased infiltrating CD3-positive cells, expression levels of IL-17A on a per-cell basis among CD3-positive cells were also significantly increased in adiponectin-deficient mice (Fig. 3e,g). Next, we gated on IL-17-positive cells and determined the cellular source of IL-17. In agreement with previous reports^{33,36}, the majority of IL-17 was produced by $\gamma\delta$ -T cells upon stimulation (Fig. 3f,h). These results suggest that adiponectin deficiency promotes the recruitment of inflammatory cells and local IL-17 production from $\gamma\delta$ -T cells in the imiquimod-induced skin inflammation.

V γ 4-positive dermal $\gamma\delta$ -T cells are the major IL-17 producers.

To determine which type of $\gamma\delta$ -T cells are involved in the dermal skin inflammation, we examined the V γ 4 and V γ 5 expression pattern of skin $\gamma\delta$ -T cells during the imiquimod treatment.

We first determined the V γ 4 and V γ 5 expression of epidermal resident $\gamma\delta$ -T cells and dermal migratory $\gamma\delta$ -T cells by reverse transcription-PCR. As shown in Fig. 4a, dermal $\gamma\delta$ -T cells expressed V γ 4, whereas epidermal $\gamma\delta$ -T cells express V γ 5, but not V γ 4. Notably, imiquimod application induced two subsets of skin $\gamma\delta$ -T cells, composed of TCR $\gamma\delta^{\text{intermediate}}$ IL-17+ (I) and TCR $\gamma\delta^{\text{high}}$ IL-17-(II) T cells in both wild-type and adiponectin-deficient mice (Fig. 4b). Consistent with the past reports^{33,37,38}, these populations expressed (I) V γ 4 and (II) V γ 5, respectively (Fig. 4c), suggesting that V γ 4-positive dermal migratory $\gamma\delta$ -T cells dominate the dermal skin inflammation and IL-17 production. In accordance with this result, when gated on IL-17-positive cell subsets, the majority of IL-17-positive cells expressed V γ 4, but not V γ 5, in both wild-type and adiponectin-deficient mice (Fig. 4d).

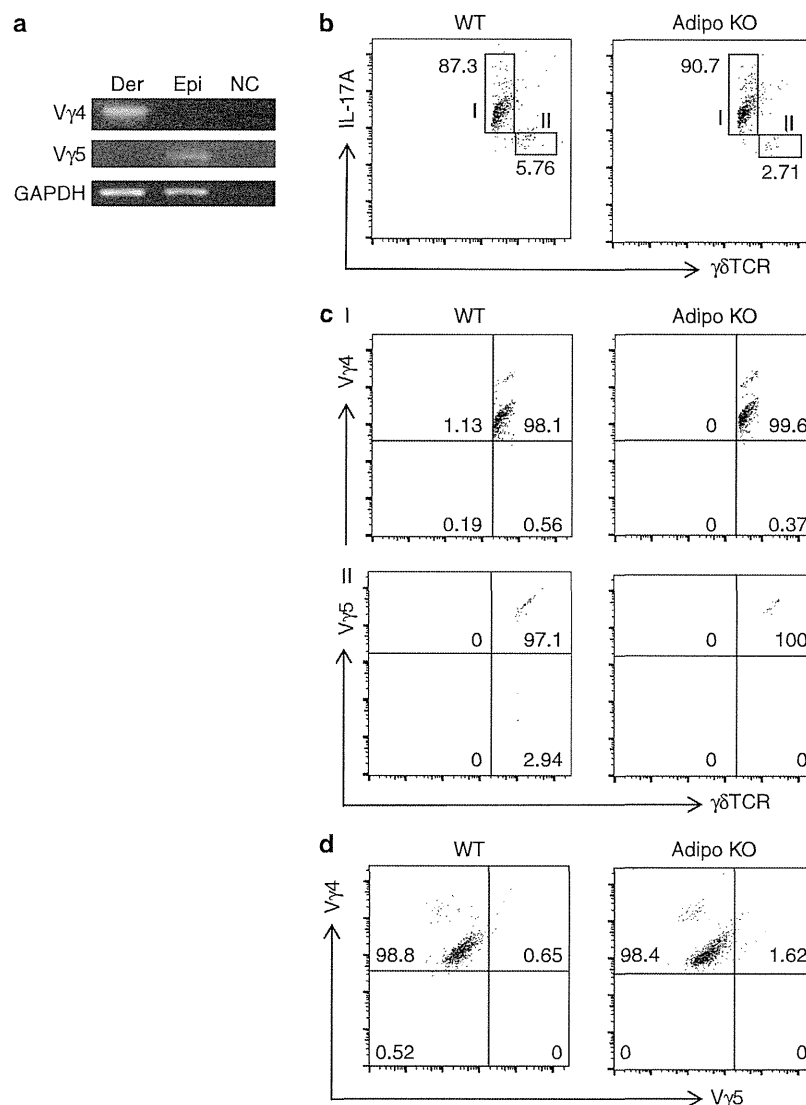


Figure 4 | V γ 4 T cells predominantly induce the skin inflammation and are the major IL-17 producers. Wild-type (WT) and Adiponectin knockout (Adipo KO) mice were treated as described. At day 5, whole-skin cell suspensions of mouse back skin were stimulated with PMA and ionomycin, and were stained with antibodies specific for IL-17A as well as CD3, TCR $\gamma\delta$, V γ 4 and V γ 5 cell surface markers, followed by flow cytometric analysis. **(a)** Dermal $\gamma\delta$ -T cells after IMQ application and epidermal $\gamma\delta$ -T cells before IMQ application were sorted, and mRNAs were extracted to perform reverse transcription-PCR. **(b)** Plots show two populations of $\gamma\delta$ -T cells, composed of TCR $\gamma\delta^{\text{intermediate}}$ IL-17-positive (I) and TCR $\gamma\delta^{\text{high}}$ IL-17-negative (II) cells. **(c)** Cells of (I) and (II) populations were characterized for TCR $\gamma\delta$ and V γ 4 or V γ 5 expression. **(d)** IL-17-positive cells gated on CD3-positive cells were characterized for V γ 4 and V γ 5 expression. Data are representative of two independent experiments, where each group contains two mice.

IL-17 regulation in $\gamma\delta$ -T cells is mediated through AdipoR1. We next focused on the *in vitro* effects of adiponectin on dermal $\gamma\delta$ -T cells. First of all, we examined the expression of adiponectin receptors, AdipoR1 and AdipoR2. It is known that AdipoR1 is expressed widely in various tissues, while AdipoR2 is predominantly expressed in the liver³⁹. As shown in Fig. 5a, western blot analysis demonstrated that only AdipoR1 protein was detected, while AdipoR2 protein expression was below the detection limit. Next, we investigated whether adiponectin had a direct effect on the production of IL-17 by $\gamma\delta$ -T cells. Sorted dermal $\gamma\delta$ -T cells were pretreated with indicated concentrations of adiponectin for 1 h, followed by treatment with IL-1 β (10 ng ml⁻¹) and IL-23 (5 ng ml⁻¹) for another 24 h, and IL-17 protein levels in the supernatant were quantified. We confirmed that adiponectin itself was not harmful by determining that IL-2 production of dermal $\gamma\delta$ -T cells is not influenced by adiponectin concentration up to 50 μ g ml⁻¹ (Supplementary Fig. 2a). Since earlier studies have revealed that $\gamma\delta$ -T cells express IL-23R and produce IL-17 in response to IL-1 β and IL-23 (ref. 40), without T-cell receptor engagement, we incubated $\gamma\delta$ -T cells without activation by anti-CD3e monoclonal antibody in this experiment. As shown in Fig. 5b, adiponectin directly

suppressed IL-17 production from dermal $\gamma\delta$ -T cells in a dose-dependent manner up to 25 μ g ml⁻¹. Consistent with the result of the supernatant protein levels, pretreatment with adiponectin (10 μ g ml⁻¹) suppressed IL-17A mRNA expression of dermal $\gamma\delta$ -T cells (Fig. 5c). Furthermore, to determine which adiponectin receptor, AdipoR1 or AdipoR2, is involved in the regulation of IL-17 synthesis, dermal $\gamma\delta$ -T cells were transfected with short interfering RNA (siRNA) against AdipoR1 and AdipoR2, and thereafter, were assessed for IL-17A mRNA expression. Quantitative real-time PCR detected both AdipoR1 and AdipoR2 mRNA in dermal $\gamma\delta$ -T cells, although AdipoR2 protein expression was below the detection limit by western blot analysis. This result is consistent with the past reports demonstrating discrepancy between mRNA and protein levels of AdipoR2 in leukocytes^{41,42}. Control experiments have revealed that AdipoR1 and AdipoR2 mRNA levels are reduced by >65% as evaluated by real-time reverse transcription-PCR analysis (Fig. 5d). We found that specific knockdown of AdipoR1, but not of AdipoR2, attenuated suppression of adiponectin-induced IL-17A gene expression in dermal $\gamma\delta$ -T cells (Fig. 5e), indicating that adiponectin suppresses IL-17 synthesis through AdipoR1 in dermal $\gamma\delta$ -T cells. Again, IL-2 expression of $\gamma\delta$ -T

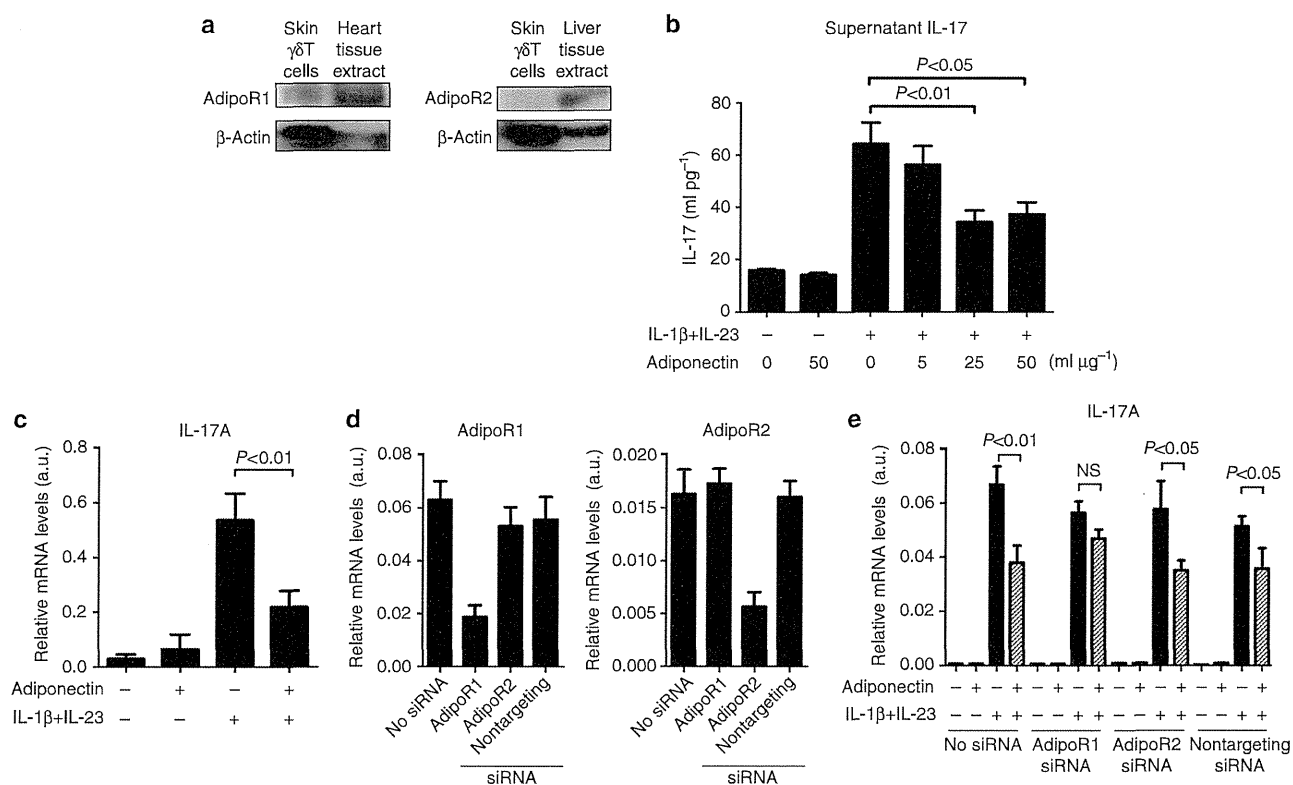


Figure 5 | Adiponectin negatively regulates IL-17 production from dermal $\gamma\delta$ -T cells through AdipoR1. (a) Sorted dermal $\gamma\delta$ -T cells were analysed for the expression of adiponectin receptors, AdipoR1 and AdipoR2. Mouse heart and liver extract were used as a positive control, respectively. (b,c) Dermal $\gamma\delta$ -T cells were pretreated with indicated concentrations of adiponectin for 1 h, followed by treatment with IL-1 β (10 ng ml⁻¹) and IL-23 (5 ng ml⁻¹) (b) for another 24 h, and the supernatant IL-17 levels were determined using the IL-17 ELISA kit ($n = 5$: cells without IL-1 β and IL-23 stimulation, $n = 6$: cells with IL-1 β and IL-23 stimulation), and (c) for another 6 h, and the gene expression levels of IL-17A was determined by quantitative (qPCR) ($n = 4$: cells without IL-1 β and IL-23 stimulation, $n = 5$: cells with IL-1 β and IL-23 stimulation). Data are mean \pm s.e. and are representative of two independent experiments. (d,e) Dermal $\gamma\delta$ -T cells were transfected with AdipoR1 or AdipoR2 siRNA or nontargeting control siRNA. After 72 h, $\gamma\delta$ -T cells were pretreated with adiponectin (10 μ g ml⁻¹) for 1 h, followed by treatment with IL-1 β (10 ng ml⁻¹) and IL-23 (5 ng ml⁻¹) for another 6 h. Messenger RNA expression of (d) AdipoR1 and AdipoR2 ($n = 8$) and (e) IL-17A ($n = 4$: cells without IL-1 β and IL-23 stimulation, $n = 6$: cells with IL-1 β and IL-23 stimulation) in transfected cells were examined by qPCR. Data are mean \pm s.e. and are representative of three independent experiments. Data are analysed by Welch's *t*-test for b,c,e. NS, not significant.

cells stimulated with IL-1 β and IL-23 was not influenced by treatment with adiponectin (Supplementary Fig. 2b).

Exogenous adiponectin rescues exacerbated dermatitis. To determine whether the exacerbation of dermatitis in adiponectin-deficient mice is particularly adiponectin dependent or not, wild-type and adiponectin-deficient mice were given daily intraperitoneal injection of adiponectin (50 μ g per day per mouse)¹⁵ from 1 day before imiquimod treatment, and the dermatitis progression and IL-17 expression were examined. Exogenous adiponectin improved imiquimod-induced dermatitis clinically and pathologically (Fig. 6a). Disease severity and ear thickness during imiquimod treatment are shown in Fig. 6b,c. Consistent with the improvement of the phenotype, exogenous adiponectin significantly suppressed elevated IL-17 production of adiponectin-deficient mice (Fig. 6d). On the other hand, additional adiponectin did not either suppress IL-17 production or improve dermatitis of wild-type mice (Fig. 6a–d). These results would suggest that the effect of adiponectin might be elicited below a certain concentration of adiponectin and that exogenous adiponectin supplementation could be effective only under the condition when adiponectin is insufficient, implying the existence of a plateau concentration that would exert biological effects *in vivo*.

Neutralization of IL-17 ameliorates exacerbated dermatitis. Finally, to assess clinical effectiveness, wild-type and adiponectin-deficient mice were intraperitoneally injected with high (80 μ g) or

low (10 μ g) doses of anti-IL-17 antibody, and then were applied imiquimod cream for 6 consecutive days. As shown in Fig. 7a, adiponectin-deficient mice with low doses of anti-IL-17 antibody injection revealed no visible phenotypic changes. In contrast, wild-type mice demonstrated phenotypical improvement with both low and high doses injection of anti-IL-17 antibody. Disease severity and ear thickness (lower panel) during imiquimod treatment are shown in Fig. 7b. Histological presentation was consistent with these phenotypes. Specifically, epidermal hyperplasia and inflammatory cell infiltration were improved in wild-type mice with both low- and high-dose injections, but in adiponectin-deficient mice with only high-dose injection (Fig. 7c).

Effects of adiponectin on human T cells. To determine whether obtained murine data are in accordance with human condition, we collected human skin and subcutaneous samples of psoriasis patients as well as controls, and compared its adiponectin level. Notably, adiponectin level of subcutaneous fat was remarkably decreased in psoriasis patients as compared with healthy controls (Fig. 8a, left panel). Furthermore, adiponectin levels of skin tissue, which locate directly above subcutaneous adipose tissue, were also significantly decreased in psoriasis patients (Fig. 8a, right panel). Adiponectin level of skin tissue significantly correlated with that of subcutaneous fat tissue in individual patients (Fig. 8b). Since conventional CD4- or CD8-positive T cells dominantly infiltrate the dermis of psoriasis patients and contribute to the formation of psoriasis plaque, we sought to examine whether adiponectin actually suppresses IL-17 production by human

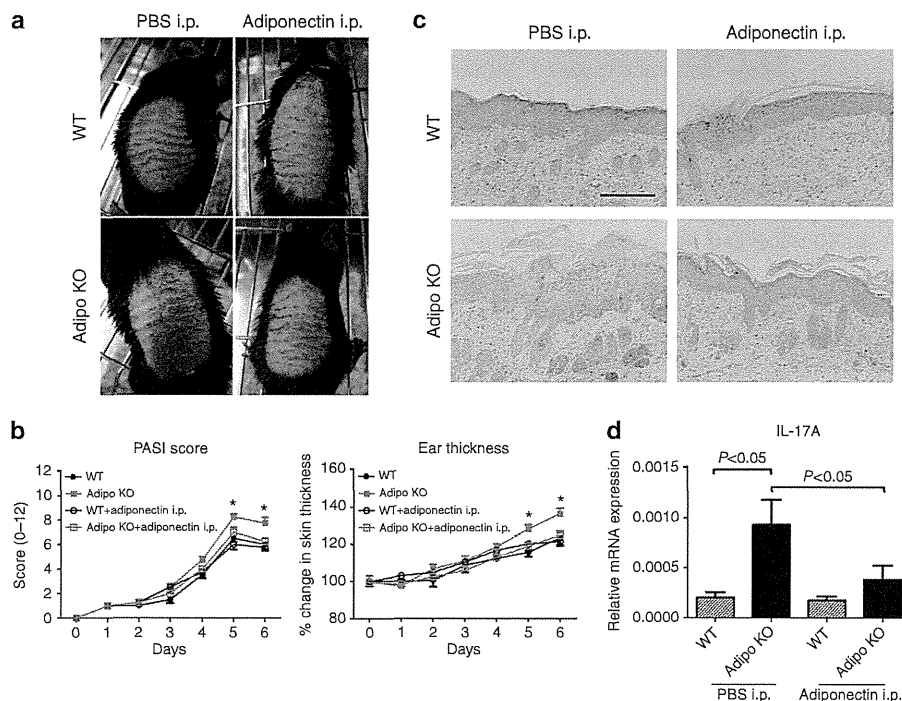


Figure 6 | Exogenous adiponectin improves the psoriasiform dermatitis in Adipo knockout (KO) mice. Wild-type (WT) and Adiponectin knockout (Adipo KO) mice were given daily intraperitoneal (i.p.) injection of recombinant adiponectin (50 μ g per day) from day 1 before imiquimod (IMQ) treatment. (a) Phenotypical manifestation of WT and Adipo KO mouse back skin induced by IMQ at day 5 with or without exogenous adiponectin administration. (b) Disease severity (left panel) and ear thickness (right panel) during IMQ treatment. Clinical scores for disease severity were calculated as described in the Methods. Data are presented as mean \pm s.e. ($n = 4$ for each group). * $P < 0.05$ versus Adipo KO mice without adiponectin administration. Data are analysed by Welch's *t*-test. (c) Histological presentation of WT and Adipo KO mouse back skin induced by IMQ at day 5 with or without exogenous adiponectin administration. Scale bar, 50 μ m. (d) IL-17 mRNA expression of WT and Adipo KO mouse back skin induced by IMQ at day 2 with or without exogenous adiponectin administration. Data are analysed by one-way analysis of variance with Dunnett's multiple comparison test.